SCHOOL OF MATERIALS AND MINERAL RESOURCES ENGINEERING
UNIVERSITI SAINS MALAYSIA

SYNTHESIS AND CHARACTERIZATION OF METAL COUPLED ZnO NANOMATERIALS WITH PLASMONIC EFFECT

By

SOO SOCK KUAN

Supervisor: Assoc. Prof. Dr. Pung Swee Yong

Dissertation submitted in partial fulfilment
of the requirements for the degree of Bachelor of Engineering with Honours
(Material Engineering)

Universiti Sains Malaysia

JUNE 2017

DECLARATION

I hereby declare that I have conducted, completed the research work and written the dissertation entitled “Synthesis and Characterization of Metal Coupled ZnO Nanomaterials with Plasmonic Effect”. I also declare that it has not been previously submitted for the award of any degree or diploma or other similar title of this for any other examining body or university.

Name of student : Soo Sock Kuan Signature:

Date : 3 July 2017

Witness by

Supervisor : Assoc. Prof.Dr. Pung Swee Yong Signature:

Date : 3 July 2017

ACKNOWLEDGEMENT

First of all, I feel grateful because School of Materials and Mineral Resources Engineering and our Dean, Prof. Dr. Zuhailawati Binti Hussain have provided us an appropriate and safe environment to us for carrying out our final year research project.

It is my radiant sentiment to place on record my best regards, deepest sense of gratitude to my supervisor, Assoc. Prof. Dr. Pung Swee Yong for his patient guidance and enthusiastic encouragement during I have carrying out my final year project. The valuable lessons learnt not only help me in enhancing my knowledge but the way to solve the problems as well.

Next, I would like to express my deepest appreciation to the technician, academic and administrative staffs for helping me in the utilization of equipment and recommendations on my final year project. They are keen in teaching and assisting me when dealing with the machines and equipment.

Last but not least, I wish to express my sincere thanks to postgraduate seniors and undergraduate friends, who are willing to guide and support me throughout my final year project.

TABLE OF CONTENTS

Contents **Page**

LIST OF FIGURES

LIST OF TABLES

LIST OF ABBREVATIONS

ALD	Atomic Layer Deposition
CVD	Chemical Vapor Deposition
DL	Deep Level
EDL	Electrical Double Layer
EDX	Energy-dispersive X-ray spectroscopy
FESEM	Field Emission Scanning Electron Microscope
FETs	Field Effect Transistors
JCPDS	Joint Committee on Powder Diffraction Standards
LEDs	Light Emitting Diodes
LSPR	Local Surface Plasmon Resonance
NBE	Near Band Edge
NPs	Nanoparticles
NWs	Nanowires
PLD	Pulse Laser Deposition
PV	Photovoltaic
PVD	Physical Vapor Deposition
RTPL	Room Temperature Photoluminescence
SPR	Surface Plasmon Resonance

ICO	In Doped in Cadmium Oxide
ITO	Tin Doped in Oxide
UV	Ultraviolet
XRD	X-ray Powder Diffraction

LIST OF SYMBOLS

k	Absorption Coefficient
O_i	Oxygen Interstitial
O_{Zn}	Oxygen Anti-Site
R_1	Absolute Diffuse Reflectance
s	Scattering Coefficient
V_O	Oxygen Vacancy
V_{Zn}	Zinc Vacancy
Zn_O	Zinc Anti-site

SINTESIS DAN PENCIRIAN NANOPARTIKAL ZINK OKSIDA KOT DENGAN METAL UNTUK KAJIAN KESAN PLASMONIK

ABSTRAK

ZnO mempunyai potensi menjadi peranti optoelektronik disebabkan jurang jalur dan tenaga mengikat yang tinggi di suhu bilik. RTPL bagi ZnO mempunyai dua puncak yang ketara, iaitu emisi NBE di kawasan UV dan emisi DL di kawasan cahaya. DL akan menurunkan intensiti NBE. Jadi, projek ini akan cari jalan untuk meninggikan emisi NBE dan menyekat emisi DL dengan berkesan. Dalam projek ini, ZnO rod submicron disintesis dengan mengguna $Zn(NO_3)24H_2O$, $(CH_2).6N_4$ dan $(C_6H_9NO)_n$ melalui kaedah sol-gel manakala ZnO nanodisks disintesis dengan mengguna $Zn(CH_3COO)_2.2H_2O$, NH_4OH and $Al_2(SO_4)_3$ melalui kaedah sol-gel. Dalam pendapatan RTPL, ZnO rod submicron mempunyai properti luminescence yang lebih bagus. Dalam bahagian kedua projeck ini, kesan kepekatan $NiNO_3$ atas ZnO rod submicron akan dikaji. Keputusan daripada RTPL menunjuk ZnO rod submicron dengan salutan 0.07 M $NiNO_3$ mempunyai properti luminescence yang paling bagus dengan I_{uv}/I_{vis} ratio: 41.15. Di bahagian terakir dalam projek ini, kesan logam (Ag, Cu, Al and Fe) yang berbeza atas ZnO rod submicron (dengan kepekatan 0.07 M) akan dikaji. Keputusan menunjuk ZnO rod submicron dengan salutan 0.07 M $NiNO_3$ mempunyai sifat-sifat luminescence yang paling bagus ikut dengan Al (I_{uv}/I_{vis} ratio 26.11), Ag (I_{uv}/I_{vis} ratio 4.44) and Fe (I_{uv}/I_{vis} ratio 4.00) manakala Cu mempunyai sifat-sifat luminescence yang paling buruk (I_{uv}/I_{vis} ratio of 0.11).

SYNTHESIS AND CHARACTERIZATION OF METAL COUPLED ZnO NANOMATERIALS WITH PLASMONIC EFFECT

ABSTRACT

Despite of its unique properties, ZnO nanomaterials have limited usage in optoelectronic devices and bio-/chemical sensor as a consequence of relatively poor UV emission. The crystal defects of ZnO that produce visible light emission is believed the origin that reduce the intensity of UV emission drastically. In this research, the enhancement of near band edge emission of ZnO particles was achieved by localized surface-plasmon resonance effect through coupling with metal nanoparticles, such as Ni, Al, Ag, Fe, and Cu. Firstly, ZnO submicron rods were synthesized via sol-gel method using $Zn(NO_3)_2.4H_2O$, $(CH_2).6N_4$ and $(C_6H_9NO)_n$, whereas ZnO hexagonal nanodisks were synthesized via sol-gel method by $Zn(CH_3COO)_2.2H_2O$, NH_4OH and $Al_2(SO_4)_3$. Since ZnO submicron rods have a better crystal quality and photoluminescent (I_{uv}/I_{vis} ratio: 1.58), they were used in subsequent phase of this project. Next, the effect of concentration of nickel nitrate on the luminescence property of ZnO submicron rods was studied. The result shows that ZnO submicron rods coated with 0.07 M $NiNO_3$ has the best luminescence property, with their I_{uv}/I_{vis} ratio: 41.15. Lastly, the luminescence properties of ZnO submicron rods deposited by Ag, Cu, Al and Fe at same molarity of 0.07 M $NiNO_3$ were compared. The result shows that ZnO submicron rods coated with 0.07 M $NiNO_3$ has the best luminescence property amongst the metals, followed by Al (I_{uv}/I_{vis} ratio 26.11), Ag (I_{uv}/I_{vis} ratio 4.44) and Fe (I_{uv}/I_{vis} ratio 4.00). The deposition of Cu deteriorated the luminescence property of ZnO submicron rods with I_{uv}/I_{vis} ratio of 0.11.

CHAPTER 1

INTRODUCTION

1.1 Research Background

Surface plasmon resonance (SPR) is a phenomenon when the conduction electrons oscillate at the boundary between a negative and positive permittivity material due to resonant, stimulated by incident light. It happens when the frequency of incident photons tally with the natural frequency of surface electrons oscillating against the restoring force of positive nuclei (Jana et al., 2016). The SPR effect has been applied in many characterization tools for quantifying adsorption of material onto planar metal (typically gold (Au) or silver (Ag)) surfaces or onto the surface of these metal nanoparticles.

Figure 1.1 shows the important research findings of surface plasmon resonance and the annual number of publications containing the words ‘surface plasmon’ in the title or the abstract (Brongersma, 2015). This could be attributed to the rapid growth of the plasmonic field is facilitated by the development and commercialization of new plasmonic materials and optical or physical analysis techniques. (Brongersma, 2015). Metal nanoparticles could enhance the performance of photo-diodes, solar cells, and silicon based photodetectors. The ultra violet radiations detection has become very crucial in commercial, military and scientific areas (Rajan et al., 2013).

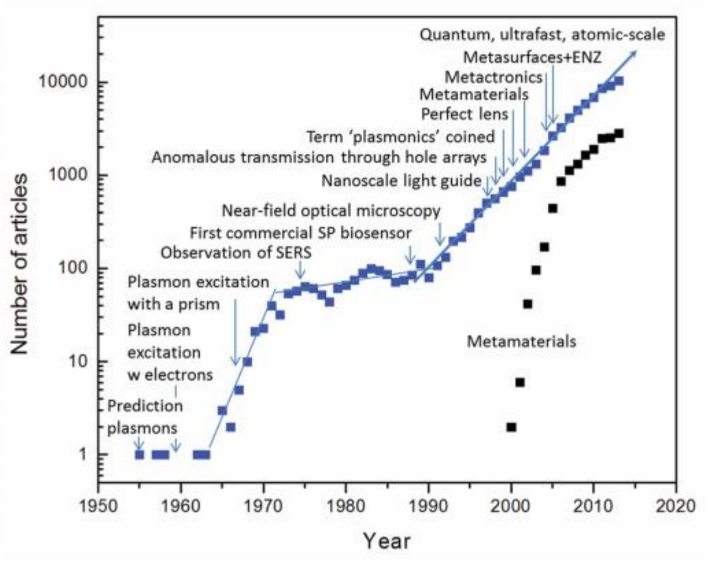

Figure 1.1: The growth of the field of plasmonic is illustrated by the number of scientific articles published annually (Brongersma, 2015).

Localized SPRs (LSPRs) are collective electron charge oscillations in metallic nanoparticles that are excited by light (Dai, 2016). They exhibit enhancement of amplitude at the resonance wavelength. The LSPR can give rise to the intense colors of suspensions or sols containing the metallic nanoparticles. In addition, these nanoparticles show intense absorption bands in the UV light region that are not existing in their bulk metal. This unique absorption has been exploited to improve light absorption in photovoltaic cells by coating metal nanoparticles on the cell surface. The wavelength of this absorption is changed when the light is polarized along or perpendicular to the nanowire. Changes in this resonance due to variations in the local index of refraction upon adsorption to the nanoparticles can also be used to identify biopolymers like DNA or proteins (Vitaliano, 2012). Figure 1.2 illustrates the schematic of LSPR where the free conduction electrons in the metal nanoparticle are driven into oscillation due to strong coupling with incident light (Hammond et al., 2014).

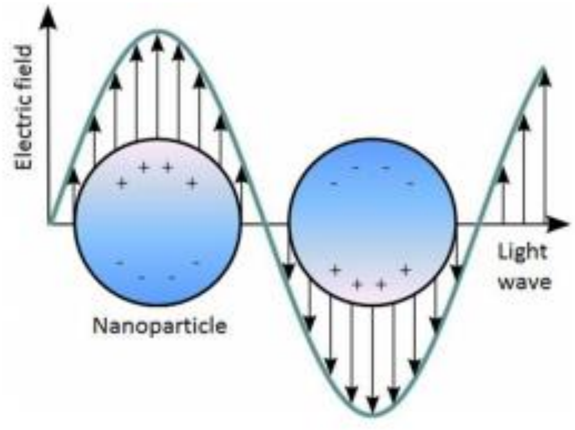

Figure 1.2: Illustration of LPSR of metallic nanoparticles (Hammond et al., 2014).

Besides using in bio-sensor, plasmonic metallic nanoparticles could be used in the applications of theranostics (Dreaden et al., 2012) and opto-electronics (Ozbay, 2006, Liu & Swihart, 2014). These metallic nanoparticles like Au or Ag nanoparticles, usually exhibit huge optical loss in the visible and near-infrared regions (Langhammer et al., 2008, Johnson & Christy, 1972) are very useful in above mentioned applications. However, the issues such as difficulty in fabricating of nano-patterns and the large magnitude of the real permittivity of Au and Ag nanoparticles are the weaknesses of using these materials in these applications. Therefore, there is a need for searching better candidates to replace metal plasmonic materials.

Amongst other plasmonic materials, transparent conductive oxides like zinc oxide (ZnO) and titanium oxide (TiO_2), are of high interests owing to their shape-dependent, tunable size-, dopant- LSPR. Particularly, metal oxide nanoparticles offer a broad window of opportunity to control and tune the shape, size and doping ratio. Furthermore, these materials, which are usually produced by solution techniques, have a bright future for fabrication of low-cost solution-based microelectronics, optoelectronic devices and solar cells (Song et al., 2014, Song et al., 2015a, Song & Zeng, 2015, Song et al., 2015b). In fact, tunable LSPR of tin doped in oxide (ITO) (Lounis et al., 2014) and In doped in cadmium oxide (ICO) (Gordon et al., 2013) NCs were reported recently.

In particular, ZnO nanomaterials, which are cheap and with good physical and chemical stability, have become a famous material among various metal oxides to be used as surface plasmonic materials (Della Gaspera et al., 2014, Saha et al., 2015, Ghosh et al., 2014). ZnO is a wide bandgap (3.37eV) semiconductor with a large exciton binding energy (60 meV) at room temperature. These unique properties make it a suitable material to be used as room temperature UV lasers (Lee et al., 2008b), solar cells (Rajan et al., 2013) and Field Effect Transistors (FETs) (Yang, 2011). In addition, the deficiency of a centre of symmetry in ZnO wurtzite structure make it possesses strong piezoelectric and pyroelectric properties. This enables ZnO in the form of NWs and nanobelts to be used as mechanical actuators and piezoelectric sensors (Lu & Wong, 2009). Moreover, the naturally high surface-to-volume ratio of quasi one-dimensional nanowires, low preparation cost, high stability, and high compatibility with microelectronic processing, have made them a candidate for chemical and biochemical sensors. For instances, making of H_2S gas sensor with single ZnO nanowires, intracellular pH sensor with ZnO nanorods and ethanol sensor with flowerlike ZnO nanostructure (Srivastava, 2014). Consequently, synthesis of ZnO nanomaterials has been of growing interest in recent years due to their wide ranging applicaions and potential commercial value.

Although the LSPR theory has been expanded from noble metals to semiconductor materials, growth of techniques to strengthen the intrinsically very weak LSPR in metal oxide is still a great challenge prior to their applications in the fields of optics, electronics, and optoelectronics applications.

1.2 Problem Statement

Attributed to its unique properties, i.e. wide direct band gap (3.2–3.4 eV) and large exciton binding energy (60 meV) at room temperature, ZnO has great potential to be used as optoelectronic devices, in particular, light emitting diodes (Bao et al., 2006, Bie et al., 2010), ultraviolet (UV) laser diodes (Lee et al., 2008b), Schottky-Barrier photodetectors (Law & Thong, 2006, Jin et al., 2008) and bio-/chemical sensor (Srivastava, 2014). As compared to thin film, ZnO nanoparticles have advantage of large surface-to-volume ratio that enhances charge transfer and light emission (Yan et al., 2009). It is also known that the room temperature photoluminescence (RTPL) spectrum of ZnO generally exhibits two characteristic emissions, i.e. near band edge (NBE) emission in the UV region and deep level (DL) (defects-related) emission in the visible region (Ma et al., 2007). The DL emission is believed to reduce intensity of the NBE emission. As a result, this limits the application of ZnO in optoelectronic devices and as bio-/chemical sensors. Therefore, it is essential to enhance the NBE emission and suppress the DL emission of ZnO effectively.

A few methods have been reported to improve the NBE emission of ZnO nanoparticles, e.g. by surface coating with polymers or oxide materials (Liu et al., 2010, Jin et al., 2011, Shi et al., 2007, Shimpi et al., 2009, Richters et al., 2008) and post-growth annealing treatment (Shan et al., 2008, Dev et al., 2010, Dev et al., 2011). Nevertheless, only a small progress has been achieved using the above methods as the enhancement of NBE emission is generally smaller than 5 folds (5 X).

1.3 Research Objectives

In this project, surface-plasmon resonance (SPR) effect was introduced to enhance the NBE emission of ZnO nanoparticles through coupling of various metal nanoparticles (NPs) such as Ni, Al, Ag, Fe, and Cu. Theoretically, the SPR coupling induced a strong localized electric field at the interface between the metal and the adjacent semiconductor. This could enhance not only the density of states but also the probability of energetic electrons transferring from the metal to the semiconductor. Thus, it improves the intensity of NBE emission of ZnO submicron rods. Thus, the objectives of this project are:

i. To synthesize and characterize ZnO submicron rods and ZnO nanodisks using sol-gel method,

ii. To synthesize and study optical properties (plasmonic effect) of Ni-, Al-, Ag-, Fe-, and Cu- ZnO submicron rods.

1.4 Project Overview

ZnO was chosen in this project as it is known for its application as chemical sensors. ZnO submicron rods were synthesized by solution precipitation method while ZnO hexagonal nanodisks were synthesized via sol gel approach. The physical properties and optical properties of these ZnO materials were characterized using field effect scanning electron microscope (FESEM), energy dispersion X-ray (EDX) analysis, X-ray diffraction (XRD) analysis, room temperature photoluminescence (RTPL) spectroscope, zeta potential analyzer and UV-Visible spectroscope. As ZnO submicron rods demonstrated a better crystal quality than ZnO nanodisks, it was used in the subsequent step.

Next, Ni was deposited on ZnO submicron rods via liquid impregnation (LI) method, followed by reduction (forming gas: 5 H_2 % + 95 N_2 %) at 500 ^{o}C. The amount of

Ni deposited onto the surface of submicron rods was varied by adjusting the concentration of nickel nitrate ($NiNO_3$) solution from 0.03 M to 0.30 M. The surface plasmonic resonance (SPR) effect of Ni-ZnO submicron rods was studied using RTPL.

Lastly, the SPR effect of Al-, Ag-, Fe-, and Cu- coupling on ZnO submicron rods was studied. These materials were prepared using the similar approach as described in previous paragraph, except using different precursors, i.e. silver nitrate ($AgNO_3$), aluminium nitrate ($Al(NO_3)_3$), iron (III) nitrate $Fe(NO_3)_3$ and copper (II) nitrate ($Cu(NO_3)_2$).

CHAPTER 2

LITERATURE REVIEW

2.1 Surface Plasmon Resonances

Surface plasmon resonance (SPR) involves the study of interaction between electromagnetic fields and free electrons in metal (Sagor et al., 2015). In this case, metals are vital in creating surface plasmon polariton. When incident light is striking on the thin metal films, it causes the collective oscillation of electrons at a resonant frequency in the metal films or nanostructures. The strong absorption or scattering of light by the metallic nanostructures will lead to occurrences like metal-enhanced fluorescence and surface-enhanced Raman scattering when coupled to fluorophores or Raman-active molecules (Lim & Gao, 2016). This phenomena could be used to probe and monitor the minor changes in the refractive index of bounding dielectric environment (Levy et al., 2015).

The study of SPR effect and its applications has attracted concern by scientists. Figure 2.1 shows the evolution of the number of publications related to surface plasmons in the Web of Science database as of 25 Mei 2017. It is noted that only 124 number of papers was published in year 2000. This number has been increased to 1028 in year 2016. In fact, SPR effect has been widely used in many applications. Deshpande (2001) summarized the applications of luminescence in life sciences as shown in Table 2.1.

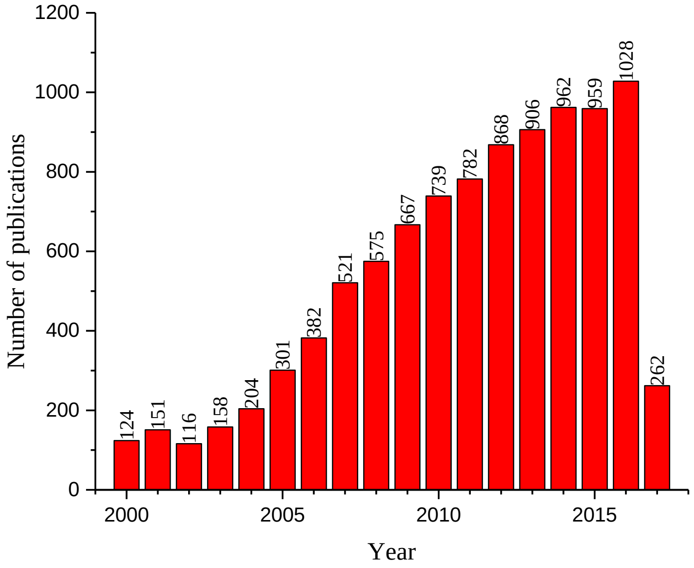

Figure 2.1: Evolution of the number of publications related to surface plasmons in the Web of Science database as of 25 Mei 2017.

Table 2.1: Applications of luminescence in life sciences (Deshpande, 2001)

Field	**Type of Analysis**
Diagnostics	Electrolytes
	Steroids
	Lipids
	Proteins
	Amino acids and metabolites
	Immunology
	Enzymes
	Drugs
	Metabolites
	Miscellaneous
Inorganic analysis	Anions
	Cations

Agriculture, food and veterinary sciences	Inorganic
	Tracing techniques
	Natural products
	Protein
	Drug residues in foods
	Toxins
	Hygiene monitoring
	Pathology
Pharmaceutical industry	Drug discovery
Public health	Pollution control
	Bacteriology
	Metal poisoning
	Immunology
	Screening programs

Localized surface plasmon resonance (LSPR), which involves of nanomaterials, display improvement of amplitude at the resonance wavelength. The metallic nanomaterials could generate intense colors of light or show intense absorption in the UV light region which is not existing in their bulk metal. This unique intensification of absorption has been exploited to increase the light absorption in photovoltaic (PV) cells by coupling metal nanoparticles on the surface of PV cell. The wavelength of LSPR depends strongly on size, shape and local dielectric environment of metallic nanoparticles (Devi & Tai, 2014). For example, Au and Ag are the commonly used plasmonic nanomaterials because they are relatively inert and offer higher carrier concentrations with limited chemical interactions (Sachet et al., 2013).

2.2 Nanomaterials

Nanoscience and nanotechnology involves of synthesis, characterization, exploration, and exploitation of nanomaterials. Nanomaterials can be classified as (a) individual nanostructures e.g. quantum dots, clusters, nanowires, nanocrystals, and nanotubes, and (b) collections of nanostructures such as arrays, assemblies, and super-lattices of the individual nanostructures. Figure 2.2 displays some of the commonly nanomaterials that reported in scientific papers.

The physical and chemical properties of nanomaterials can vary significantly from those of bulk materials of the same composition. In fact, by suitable control of the size, one can alter the properties of nanomaterials remarkably and make possible new devices and technologies (Gogotsi, 2006). For instances, the particles size of material has great effect on its physical and chemical properties. The decrease in the particle size will result in the increase in surface to bulk atom ratio and surface area. This results in an increase in the oxidation and reduction ability of the nanomaterials. The higher specific surface area-to-volume ratio of nanoparticles may display better performance in the degradation of organic pollutants than bulk ones (Bagnara et al., 2016).

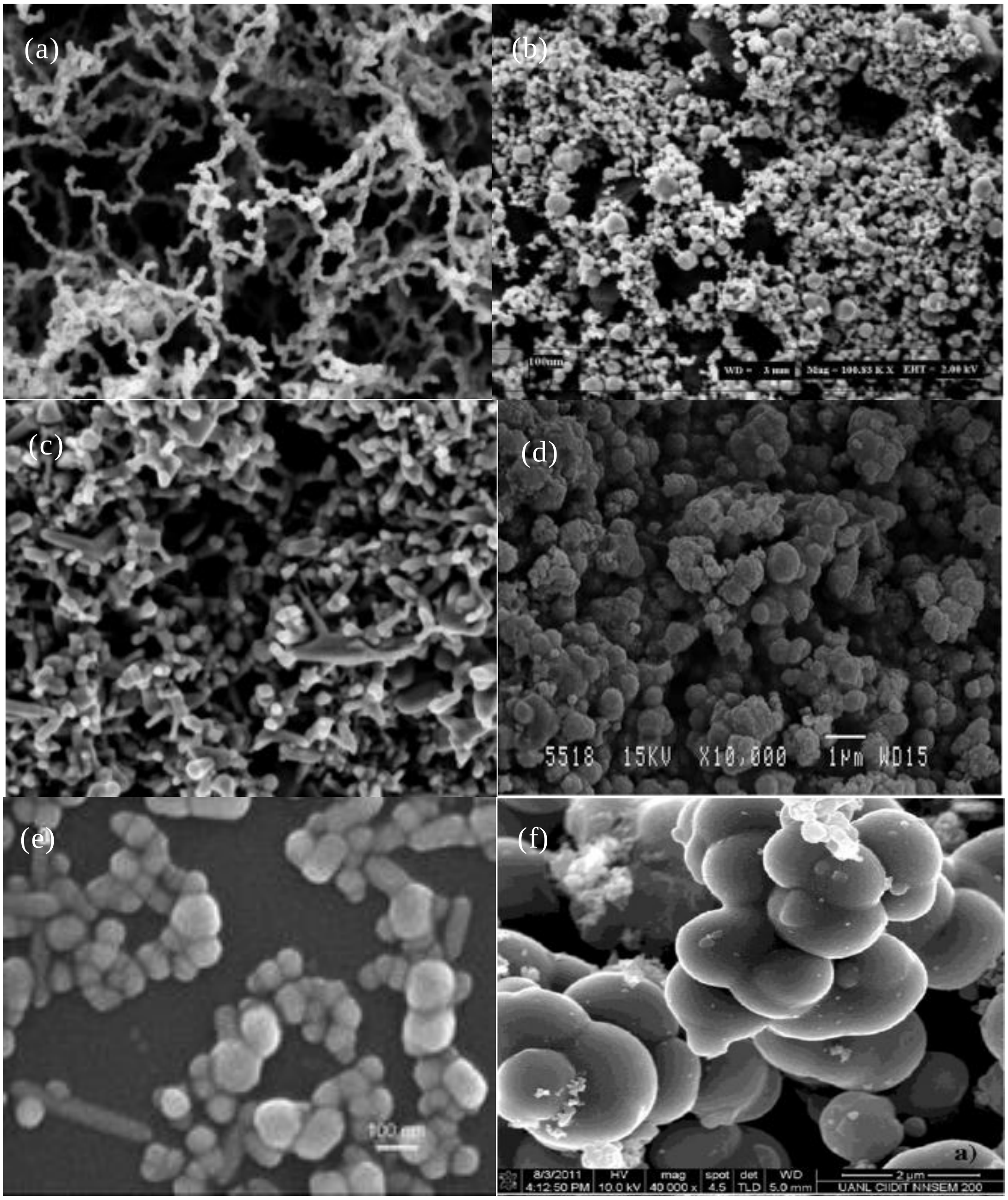

Figure 2.2: Various types of nanomaterials (a) Cobalt (Pitkethly, 2004), (b) Copper oxide (Pitkethly, 2004), (c) Silver (Pitkethly, 2004), (d) Iron oxide (Hallam et al., 2012), (e) Gold (Xu et al., 2009), (f) Titanium oxide (Ramos-Delgado et al., 2013).

In addition, the reduction in the particles size could alter the band gap of semiconductors. It will then shift the light absorption and emission towards the high energy region (blue shift). As shown in Figure 2.3, the UV-Vis absorption spectra of Ag have been shifted to a smaller wavelength with the reduction of particle size (Saion et al., 2013). The recombination rate of photo-excited electron-hole pairs is reduced significantly (Viswanathan, 2009). On the other hand, Figure 2.4 shows the effect of particle size quantization on the emission of light of Au colloids (Ghoshal et al., 2011).

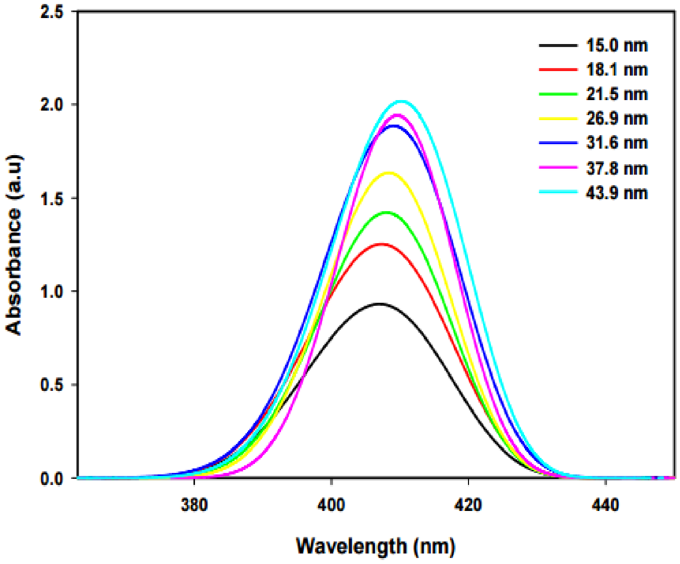

Figure 2.3: Shift of UV-Vis absorption spectra of Ag with reduction of particle size (Saion et al., 2013).

Figure 2.4: The effect of Au particle size quantization, i.e. the smallest particles emit violet color and the largest emit red color (Ghoshal et al., 2011).

Nanoparticles exhibit remarkable optical and electronic properties when compared to their bulk structures. This is because of the photoluminescence from nanomaterials are much higher (~10^{-4}) than a bulk noble metal (only near to 10^{-10}). For example, the photoluminescence efficiency of Au and Ag nanoparticles is enhanced by 6 to 7 orders of magnitude. This enhancement in photoluminescence efficiency are attributed to quantum confinement (Ghoshal et al., 2011) as illustrated in Figure 2.5. Figure 5 shows the correlation between free dimensions and density of states (DOS) of semiconductors (SC) Quantum confinement happens when the nanocrystal radius becomes comparable to the bulk exciton Bohr radius (Nirmal & Brus, 1999). The photo-exited electron-hole pairs (Mott-Wannier excitons) in these nanoparticles behaves similarly like the hydrogen-like bound state between the proton and the electron of the hydrogen atom (Chin, 2008). Consequently, they are found to be an excellent fluorescent probes for signaling, imaging, evolution and targeting of cells, attributed to their capability of emitting color during absorption of light. Thus, these nanomaterials can function as indicators or sensors for bio-molecules (Viswanathan, 2009). They should be able to distinguish the presence and absence of a certain bio-molecules by producing different absorption characteristic.

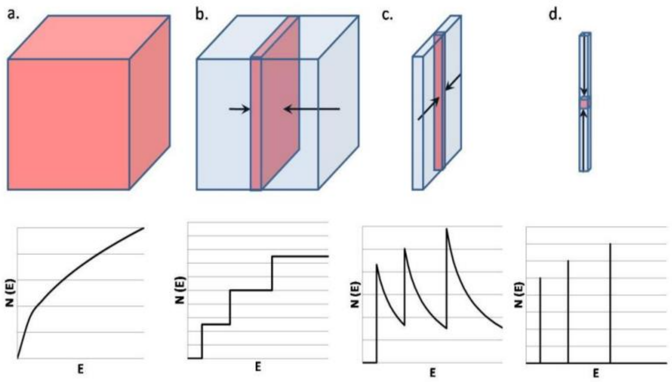

Figure 2.5: The correlation between free dimensions and density of states (DOS) of semiconductors (SC) (a) 3D system, known as bulk SC, (b) 2D system, known as Quantumwell, (c) 1D system, known as Quantum wire and (d) 0D system known as Quantum dot (Yaacobi-Gross, 2012).

2.3 Zinc Oxide

ZnO is a semiconductor material that has been studied since 1912. In early day, it is used as an important additive to the rubber of car tyres. It facilitates the vulcanization process and helps in dissipating heat when the tyre contacts the ground. Other conventional applications of ZnO are as additive in concrete for pro-longing the processing time and improves the resistance of concrete against water; as UV-blocker in sun lotions and as an additive to human and animal food. In the mid 1990s, considerable research have been done particularly in the synthesis of various ZnO thin films and nanomaterials such as epitaxial layers, nanowires or quantum dots. These ZnO nanomaterials could be used for various potential applications e.g. blue/UV optoelectronics, radiation hard material for electronic devices in a hostile environment, and as ferromagnetic material (doped with Co, Mn, Fe, V or similar elements) for semiconductor spintronics.

2.3.1 General Properties

ZnO is a wide bandgap semiconductor. It has a direct band gap of 3.37 eV and binding energy of 60 meV at room temperature (Liu et al., 2013). The excitons of ZnO are thermally stable at room temperature due to its extreme high exciting binding energy, i.e. 60 meV (Bai et al., 2016). It is a superior optoelectronic material, which is widely used in gas sensor, optical detector, solar cell, short-wavelength UV laser, as well as optoelectronic material (Lee et al., 2008b). Attributed to its wide bandgap (3.37 eV), pure ZnO has transmittance of more than 75% and low absorption and scattering values, making it transparent over the visible range (Shemis et al., 2014). In addition, ZnO is an intrinsic n-type semiconductor with good electron mobility with 2000 cm^2 at 80 K (Thandavan et al., 2015).

2.3.2 Crystal Structure

Generally, three different types of ZnO crystal structures could be found, i.e. zinc blende, rocksalt (Rochelle salt) and hexagonal wurtzite. The zinc blende and rocksalt ZnO crystal structures are illustrated in Figure 2.6 (Jagadish & Pearton, 2011). The zinc blende structure of ZnO can only be produced by growing on a cubic substrate in order to get a stable phase. On the other hand, the ZnO cubic rocksalt structure is only obtainable at high pressure (~10 GPa).

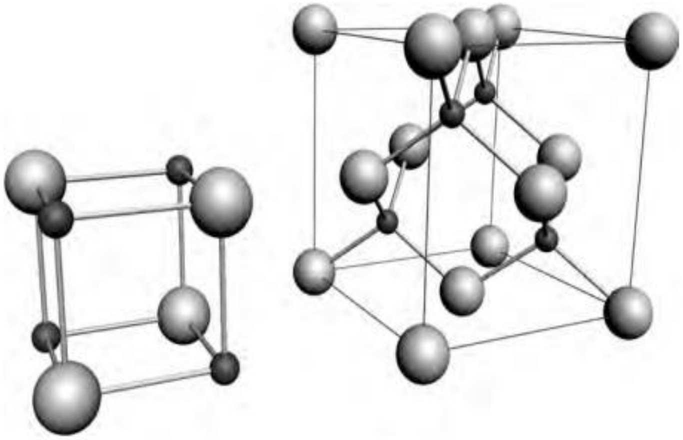

Figure 2.6: The rock salt (left) and zinc blende (right) phases of ZnO. O atoms are shown as white spheres, Zn atoms as black spheres. Only one unit cell is illustrated for clarity (Jagadish & Pearton, 2011).

The hexagonal wurtzite is the most thermodynamically stable phase of ZnO at ambient condition (Alvi, 2011). As shown in Figure 2.7, each zinc atom is surrounded by 4 oxygen atoms, which are located at the corners of a nearly regular tetrahedron. This crystal structure is composed of two interpenetrating hexagonal-closed-packed sub-lattices. Each of sub-lattices consists of either Zn^{2+} ions or O^{2-} ions displaced with respect to each other along the *c*-axis. The zinc-oxygen spacing along the c axis (~0.190 nm) is slightly shorter than that of the other Zn–O bonds (~ 0.198 nm) (Rodnyi & Khodyuk, 2011). The lattice parameters of the hexagonal wurtzite ZnO are a = 3.2495 Å and c = 5.2069 Å, and the density is 5.605 g cm^{-3}.

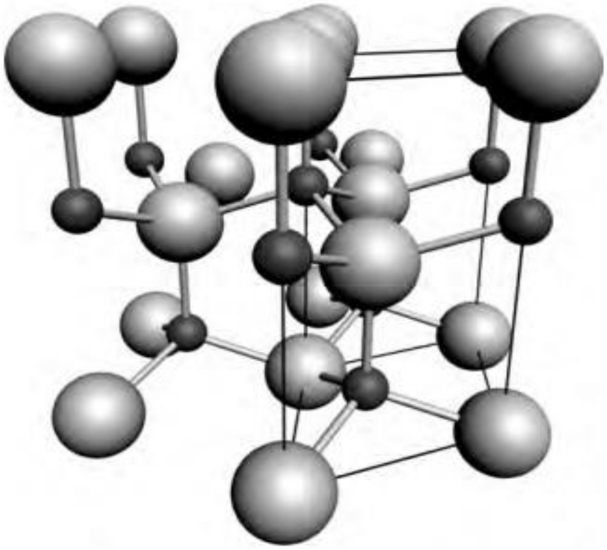

Figure 2.7: The hexagonal wurtzite structure of ZnO. O atoms are shown as large white spheres, Zn atoms as smaller black spheres. One unit cell is outlined for clarity (Jagadish & Pearton, 2011).

Since ZnO belongs to wurtzite structure family, it has three fast growth directions i.e, [0001], ±$[01\bar{1}0]$, ±$[10\bar{1}0]$, ±$[1\bar{1}00]$, ±$[2\bar{1}\bar{1}0]$, ±$[\bar{1}2\bar{1}0]$ and ±$[\bar{1}\bar{1}20]$. Thus, a big group of ZnO nanostructures could be synthesized by tuning the growth rates along these directions using different choice of precursors, substrate temperatures, type of catalysts, oxygen contents, and pressures. Figure 2.8 shows a diverse group of ZnO nanostructures reported by researchers.

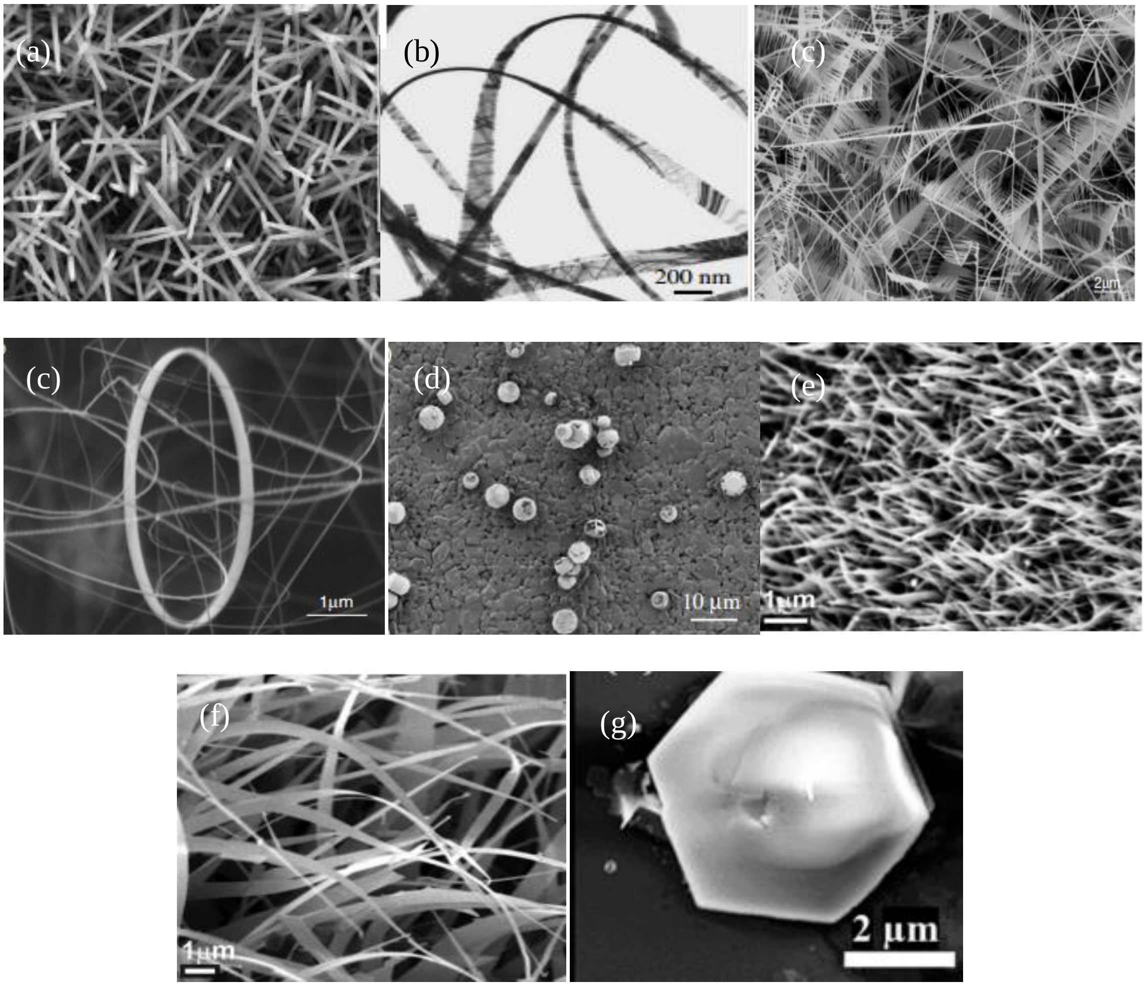

Figure 2.8: Various types of ZnO nanostructures (a) nanorod (Wang, 2004), (b) nanobelt (Wang, 2004), (c) nanocomb (Wang, 2004) (d) nanoring (Wang, 2004) (e) nanocage (Wang, 2004) (f) nanowire (Dhara & Giri, 2011) , (g) nanoribbon (Dhara & Giri, 2011) and (h) nanodisks (Alenezi et al., 2014).

Amongst these nanomaterials, ZnO nanorods and ZnO nanodisks are two important crystal structures attributed to its unique build up. Figure 2.9 shows the schematic of hexagonal wurtzite ZnO rod and disk structures. The [0001] axis (noted *c*-axis) is pointed from the face of the O-plane to the face of the Zn-plane. Other surfaces are non-polar surfaces. These non-polar surfaces are relatively stable. In addition, the crystal planes perpendicular to the *c*-axis are either positively Zn-terminated (0001) surface or negatively O-terminated ($000\bar{1}$) surface. The physical and chemical properties of these polar surfaces are different as compared to other non-polar crystal planes such as $\{01\bar{1}0\}$. Thus, these surfaces and morphology could affect the photocatalytic performance of ZnO nanostructures (Tian et al., 2011).

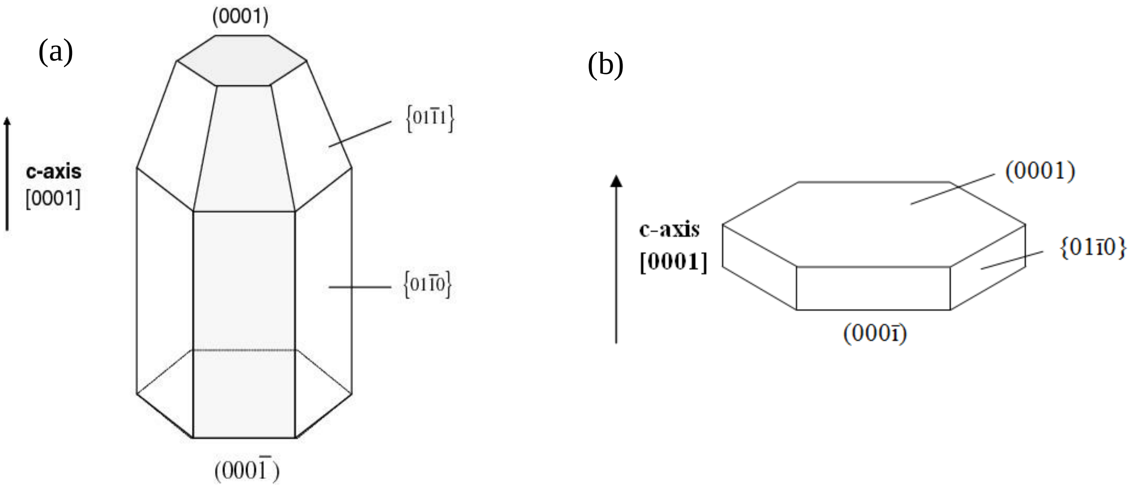

Figure 2.9: Zn-terminated (0001) and O-terminated $(000\bar{1})$ surface of hexagonal wurtzite (a) ZnO rod-like structure (Pauporté, 2009) and (b) ZnO disk-like structure (Zhang et al., 2008).

2.3.2.1 ZnO Nanorods

In current years, ZnO nanorods have been receiving particular attention due to their valuable properties. They are very important in environmental and bio-industries. The advantages of ZnO nanorods compared to other shape are their small size, possesses polar surface and being bio-safe to facilitate the chemical sensing process. Besides, they are non-toxicity, high chemical stability, high electrochemical activity, and high electron communication features make them useful in chemical and biological application (Asif, 2009). ZnO nanorods are potential candidate in sensing different types of reducing gases (Xu et al., 2000). Numerous chemical, electrochemical and physical deposition techniques have been used to generate oriented arrays of ZnO nanorods, such as catalytic growth via the vapor–liquid–solid epitaxial mechanisms, metal-organic chemical vapor deposition, pulsed laser deposition and templating with anodic alumina membranes (Mehrabian et al., 2013).

2.3.2.2 ZnO Nanodisks

ZnO nanodisks have potential applications in whisper gallery mode lasers, information storage, transducers, light emitters, and sensors. However, due to its highly anisotropic growth character of ZnO along the c-axis, the preparation of two-dimensional ZnO nanodisks remains a significant challenge(Jin et al., 2012). Until today, only a few papers are involved in the preparation of ZnO nanodisks. ZnO nanodisks are hexagonal nanoplates with high facet population and $\{011\bar{0}\}$ side face. ZnO nanodisks with circular column-based thin disks are seldom reported (Jin et al., 2012).

The catalytic behavior of ZnO nanodisks with high (0001) is always being compared with ZnO nanorods. If the plates grow too thick, the plates have a tendency to grow into prisms. Then, the catalytic effect of facets nearby the plates cannot be totally excepted. Hence, the synthesis of single-crystalline nanodisks with comparable dimension with that of nanorods for the comparison of facet related catalytic performance is still a difficult task. Compared with hexagonal plates even with thick plates, the suppression of characteristic facets perpendicular to (0001) facet of the nanodisks will lessen the effect other than (0001) facet to the minimum during the comparison of photocatalytic activities, which is another progression for the synthesis of the special single-crystalline ZnO nanodisks (Zeng et al., 2009).

ZnO nanodisks with high (0001) population show superior photocatalytic reactivity to that of nanowires despite of nanodisks' smaller surface area. Figure 2.10 below shows the schematic illustration of the growth models for nanodisks (Zeng et al., 2009).

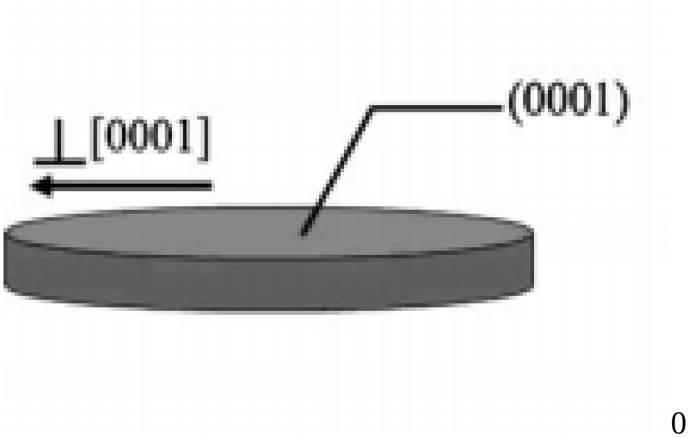

0

Figure 2.10: Schematic illustration of the growth models for nanodisks (Zeng et al., 2009).

2.3.3 Optical Properties

ZnO is a strong luminescent material. It is being developed as optoelectronic device that is environmental friendly because of its non-toxic nature (Willander et al., 2009). In a typical room temperature photoluminescence (RTPL) measurement, the luminescence starts from transition of electrons from a completely filled d band (valence band) of ZnO which is the highest occupied molecular orbital to the unoccupied levels in the *s-p* band (conduction band) which is lowest unoccupied molecular orbital. The emission happens when the direct recombination of conduction electrons with holes in the *d* bands of the quantum confined structures occur. Other emission bands may also appear due to the radiative intra-band transitions within the s-p band across the band gap.

Figure 2.1 shows a typical room temperature photoluminescence (RTPL) of ZnO material (Kashif et al., 2013). Generally, it consists of two characteristic emissions, i.e. near band edge (NBE) emission in the UV region and deep level (DL) (defects-related) emission in the visible region. The DL emission is attributed to the extrinsic and intrinsic deep-level impurities (defects) that emit different color of light like violet, blue, green, yellow, orange and red that constituent of white light during RTPL measurement. The UV emission in ZnO will only disappear when the excitation energy is lower than its band gap energy or if the intensity of visible emission is too high due to the high defect density (Kundu et al., 2011). In another words, the DL emission is believed to reduce intensity of the NBE emission.

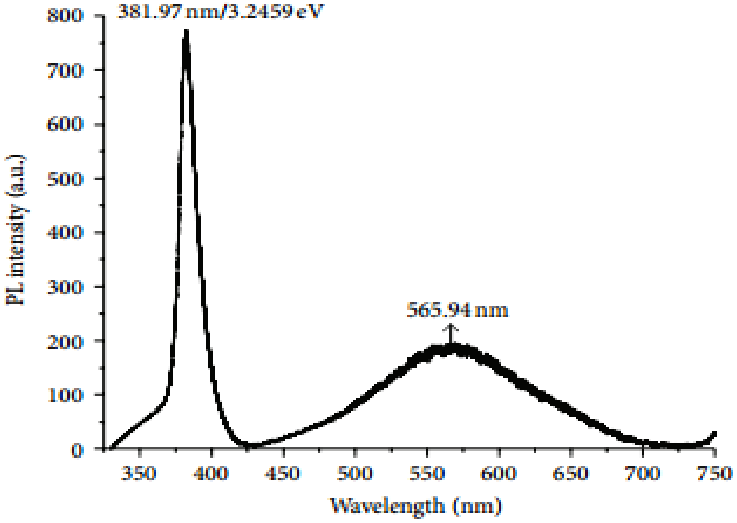

Figure 2.11: A typical RTPL of ZnO nanorods which composes of two emission peaks, i.e. NEB emission and visible light emission (Kashif et al., 2013).

If the transition level is likely ionized at room temperature or the operating temperature, then this is called a shallow transition level. In contrast, it is called deep transition level (Willander et al., 2010). The deep levels of ZnO can be divided into extrinsic and intrinsic deep levels. The possible intrinsic 'native' deep levels that happened in ZnO are oxygen vacancy (V_O), zinc vacancy (V_{Zn}), oxygen interstitial (O_i), zinc interstitial (Zn_i), oxygen anti-site (O_{Zn}), and zinc anti-site (Zn_O) (Willander et al., 2010). On the other hand, extrinsic deep levels such as donors and acceptors could be generated by doping. They induced energy levels close to conduction and valence bands (Janotti & Van de Walle, 2007).

Kundu et al. (2011) stated that the violet luminescence emission is due to the transition from conduction band to the deep holes trapped levels such as V_{Zn} while the blue luminescence emission is due to the direct recombination of conduction electron in the Zn 3d band and a hole in the O 2p valance band. He also proposed that the green emission is due to two different mechanisms, either the transition from near conduction band edge to deep acceptor level or from deep donor level to valence band. He illustrated his findings in Figure 2.12.

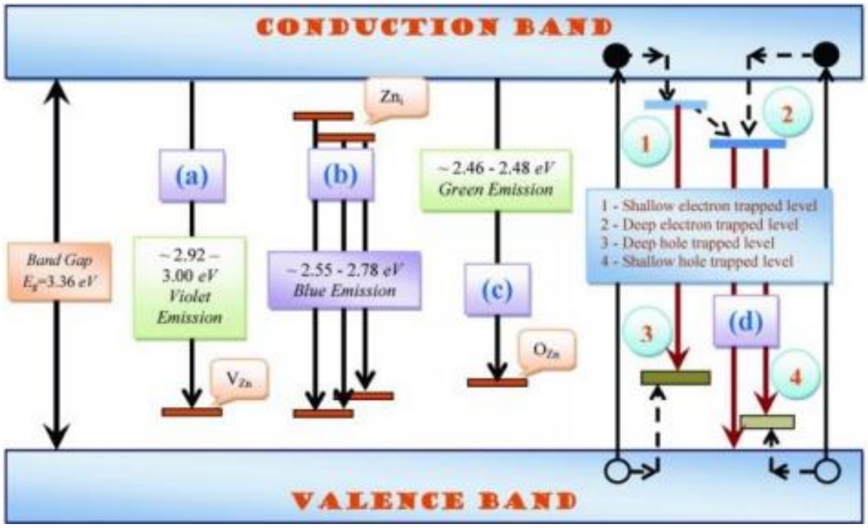

Figure 2.12: Schematic view of the energy band diagram of zinc oxide (Kundu et al., 2011).

Similarly, Willander et al. reported that (Willander et al., 2010) the yellow luminescence emission was observed in zinc oxide nanorods. The blue luminescence emission in ZnO belongs to V_{Zn} where the recombination between Zn_i energy level to V_{Zn} energy level happened while the red luminescence emission attributed to doubly ionized oxygen vacancies. However, Djurišić et al. (2007) proposed the red luminescence emission is due to the $Zn_{i.}$ Figure 2.13 shows a schematic diagram of the different energy levels of the different deep-level defects reported by different groups while Table 2.2 summarizes the different colors observed that their associated deep-level defects (Willander et al., 2010). The + and – symbols represent charged deep levels. 3 shallow levels are also shown due to neutral oxygen vacancies, positively charged extrinsic hydrogen, and neutral zinc interstitials. In addition, the position of the deep level due to V_OZn_i clusters is indicated.

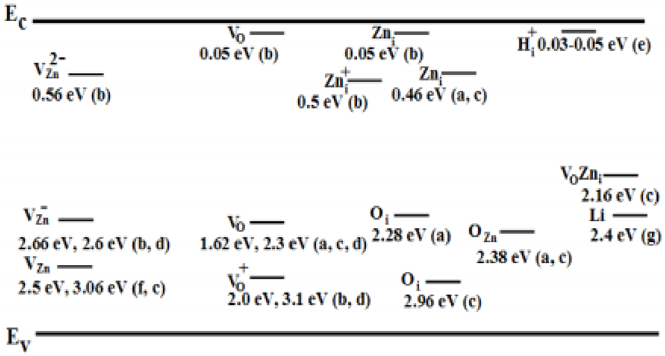

Figure 2.13: Energy levels of the different deep level defects in ZnO reported in the literature by different groups (Willander et al., 2010).

Table 2.2: Different colors observed their associated deep-level defects and the proposed associated deep level defect(s) causing the emission (Willander et al., 2010).

Emission color (nm)	Proposed deep level transition
Violet	Z_{ni} to V.B.
Blue	Zni to V_{Zn} or C.B. to V_{Zn}
Green	C.B. to V_O, or to V_{Zn}, or C.B. to both V_O and V_{Zn}
Yellow	C.B. to Li, or C.B. to O_i
Orange	C.B. to O_i or Z_{ni} to O_i
Red	Lattice disorder along the c-axis (i.e. due to Zni)